Thongsamer *et al.*
Sustainable Environment Research (2022) 32:39
https://doi.org/10.1186/s42834-022-00150-x

Sustainable Environment Research

RESEARCH

Open Access

Chitosan impregnation of coconut husk biochar pellets improves their nutrient removal from eutrophic surface water

Thunchanok Thongsamer[1], Soydoa Vinitnantharat[1,2], Anawat Pinisakul[3*] and David Werner[4]

Abstract

The presence of excess nutrients in water resources can be harmful to human health and aquatic ecosystems. To develop an affordable water treatment method, the agricultural waste material coconut husk was converted into a low-cost adsorbent by thermal conversion to biochar, pelletized without (CH), and with chitosan (CHC), or eggshell powder (CHEG) modifications. The physical and chemical properties of all adsorbents were characterized using Brunauer-Emmett-Teller (BET) surface analysis, Fourier transform infrared spectroscopy, scanning electron microscopy, pH_{zpc}, iodine number and elemental analysis. The adsorption of ammonium (NH_4^+), nitrate (NO_3^-), and phosphate (PO_4^{3-}) in single and mixed solute solutions was investigated for initial concentrations of 10 mg L^{-1}. Langmuir, Freundlich, Sips, Dubinin-Radushkevich (D-R) and BET isotherm models were used to investigate the adsorption mechanisms. The maximum adsorption capacity of NH_4^+ on CH, CHC, and CHEG from mixed solute solution was 5.0, 4.7 and 5.9 mg g^{-1}, respectively, while the adsorption capacity of mixed:single solute solution was 0.95, 0.93, and 1.04, respectively. CH, CHC, and CHEG had greater ability to remove the cation NH_4^+ than anions NO_3^- and PO_4^{3-} from aqueous solution. The highest maximum adsorption capacity for anions NO_3^- and PO_4^{3-} was found on CHEG (1.7 mg g^{-1}) and CH (6.7 mg g^{-1}), respectively. NH_4^+ and NO_3^- were bound by chemisorption as indicated by D-R isotherm *E* values (> 8 kJ mol^{-1}), and enthalpy ΔH values (> 80 kJ mol^{-1}). In contrast, PO_4^{3-} adsorption was mainly by physical interaction, including pore-filling, and electrostatic attraction. Pseudo first order and pseudo second order models provided good fits of the sorption kinetics data ($R^2 > 0.9$). The initial concentrations of NH_4^+, NO_3^-, and PO_4^{3-} in surface water sampled from a canal in Bangkok were 10.4, 1.2, and 3.9 mg L^{-1}, respectively, which indicated eutrophication. At a dose of 20 g L^{-1}, CHC achieved the best nutrient removal from this surface water, by 24% for NH_4^+, 25% for NO_3^-, and 66% for PO_4^{3-} after 48 h contact, respectively.

Keywords: Eutrophication, Water treatment, Biochar, Adsorption, Nutrient removal

1 Introduction

Nitrogen and phosphorus are the main elements causing surface water eutrophication. Eutrophication occurs when the total N and P concentrations in surface water exceed 1.5 mg-N L^{-1} and 0.75 mg-P L^{-1}, respectively [1]. Eutrophication stimulates aquatic plant and algae growth, leading to an imbalanced aquatic ecosystem, oxygen depletion, and production of cyanotoxins which pose a risk to human and ecosystem health. Inorganic nutrients exist mainly in the forms of ammonium (NH_4^+), nitrate (NO_3^-), and phosphate (PO_4^{3-}). For combinations of these ions, it was found that NH_4^+ with PO_4^{3-} has greater effect on phytoplankton growth than NO_3^- with PO_4^{3-} [2]. The primary source of nutrient pollution in water resources is untreated domestic

*Correspondence: anawat.pin@mail.kmutt.ac.th

[3] Chemistry for Green Society and Healthy Research Group, King Mongkut's University of Technology Thonburi, Bangkok 10140, Thailand
Full list of author information is available at the end of the article

wastewater and runoff from agriculture, affecting fisheries and raw water used for aquaculture [3]. Also, water supply is often based on raw water abstraction from a river, pond, lake, reservoir, or groundwater, and high nitrate levels in drinking water can disturb oxygen transport in the bloodstream, consequently affecting infants at risk for methemoglobinemia, or blue baby syndrome [4]. The allowable NO_3^- concentration for drinking water set by the World Health Organization (WHO) is $50\,mg\,L^{-1}$ equivalent to $11.3\,mg\,N\,L^{-1}$. In a nutrient-rich environment, cyanobacteria can quickly create algae blooms that release cyanotoxins into water. The occurrence of cyanotoxins is another threat to drinking water resources, and the WHO has set a preliminary guideline for microcystin in drinking water of $1.0\,\mu g\,L^{-1}$ [5].

Conventional water treatment uses a coagulation/clarification process which is not effective in removing inorganic nutrients. Activated carbon (AC) filtration processes are also widely used for water purification, but AC is a high-cost adsorbent. Alternatively, biochar from agriculture residues has recently been promoted as a low-cost adsorbent and waste valorization opportunity in a circular economy [6]. Biochar can be produced by thermal conversion of biomass under oxygen-limited conditions. Biochar is an effective adsorbent to bind contaminants in soil and water [7] due to the porous and surface properties of biochar which facilitate pollutant adsorption. The application of biochar to adsorb pollutants from the water is attractive and the numbers of related research studies is rapidly increasing [7–9]. Biochar and modified biochar are effective materials to adsorb NH_4^+ [10, 11]. Typically, biochar has a negative charge on the surface which effectively adsorbs NH_4^+, but negligibly adsorbs NO_3^- and PO_4^{3-} because of charge repulsion. This deficiency can be addressed with biochar modifications. Biochar composites with eggshell powder [12] or Mg-Al [13] have the potential to adsorb NO_3^-. Also, chicken-eggshell contains calcium and magnesium cations and has capacity for NO_3^- adsorption at $2.8\,mg\,g^{-1}$ [12]. Modified biochars can also enhance PO_4^{3-} adsorption [13, 14]. Chitosan is another environmentally friendly material that is available from agricultural waste like shrimp shells, and effectively adsorbs inorganic anions in water due to the amine functional groups (R-NH_3^+). Zhao and Feng [15] reported that chitosan microspheres can remove NO_3^- and PO_4^{3-} with an adsorption capacity of 32.2 and $33.9\,mg\,g^{-1}$, respectively. Chitosan coated biochar could thus potentially facilitate the NO_3^- and PO_4^{3-} adsorption from aqueous solution. Moreover, biochar with Mg and Ca contents has a great capacity for PO_4^{3-} adsorption, as reported by Almanassra et al. [16].

Biochar is typically used as an adsorbent in powdered form or small aggregates. However, powder is not suitable for adsorption filters as it clogs easily. Using biochar pellets as media in the filtration process for wastewater treatment would reduce such detrimental head loss. Pelletization of biochar can be done by mixing biochar with a binder such as starch, molasses, rubberwood, or chemical reagents. Hu et al. [17] found that starch could be used as a binder with good hydrophobicity but lower mechanical strength than NaOH. Aransiola et al. [18] found that using cassava starch, corn starch or gelatin at 10–30% (w/w) as binders produced biochar briquettes of storable stability. Therefore, using a starch solution with a pellet machine is a promising technology for biochar pellets production.

In most previous studies, adsorption studies were carried out as single solute batch adsorption experiments, which are difficult to extrapolate to field conditions [9]. Many pollutants and ions coexist in the water system, significantly influencing the equilibrium adsorption capacity [8]. Furthermore, most nutrient adsorption studies were conducted with high initial concentrations that are unrealistic in environmental remediation applications. For applications of biochar to remove nutrients from surface water, lower initial nutrient concentrations should be used for adsorption studies.

The aims of this study were: (i) to investigate the properties of biochar pellets produced from coconut husk biochar with and without surface modification; (ii) to establish the adsorption mechanisms of the three key nutrients (NH_4^+, NO_3^-, and PO_4^{3-}) by these biochar pellets in single solute and mixed solute solutions with environmentally relevant initial concentrations; (iii) to investigate the effect of initial pH on nutrient adsorption; and (iv) to demonstrate the application of these biochar pellets to the treatment of nutrient polluted surface water.

2 Materials and methods

Coconut husk was obtained from central Thailand and carbonized to biochar by a community 200-L drum kiln method at a temperature of around 400 °C [19]. The carbonized husks were crushed to powder and used for making three types of biochar pellets as summarized in Fig. 1.

2.1 Biochar and pelletization

Commercial corn flour (McGarrett) was used as a binding agent for biochar pelletization. To make a gelatinized starch, 10 g of corn flour was thoroughly mixed with 100 mL deionized (DI) water and boiled until the solution was a viscous liquid. The liquid was mixed with 50 g of coconut husk biochar powder and agitated until a homogeneous mixture was observed. The mixture was processed by a pellet mill with diameter of 4 mm,

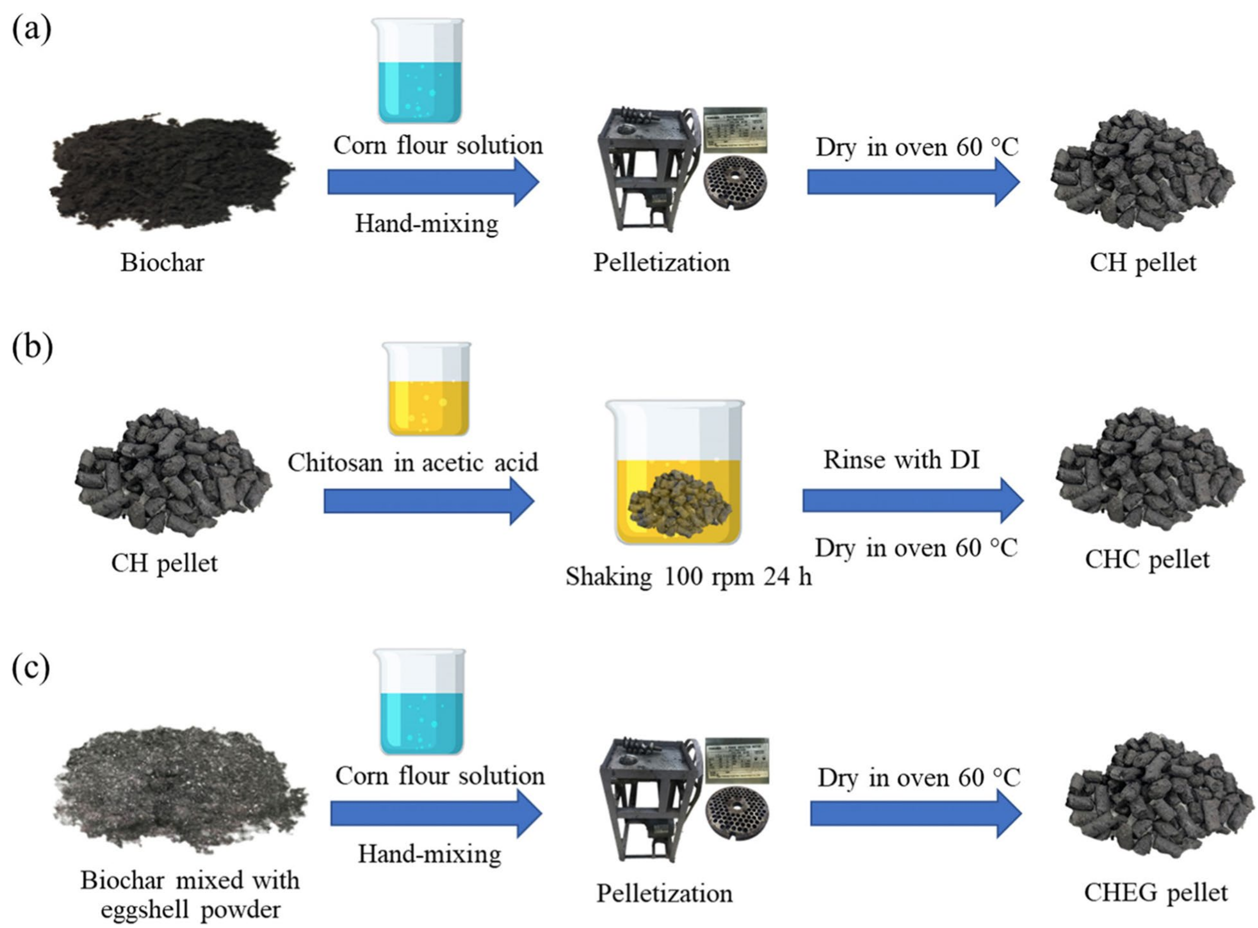

Fig. 1 Diagram of (**a**) coconut husk biochar pelletization and its modification with (**b**) chitosan and (**c**) eggshell powder

the pellets were cut into 5–10 mm lengths and dried in the oven (AS ONE, OFW-600B) at 60 °C for 24 h. The coconut husk biochar pellets (CH) were kept in a plastic bottle in a dry place and used for all experiments.

2.1.1 Chitosan coating of biochar pellets

Shrimp chitosan powder provided from Biolife ELAND, Thailand, was used to coat CH pellets (CHC). Five grams of chitosan powder were placed in a 250 mL glass bottle containing 500 mL of 1% (v/v) acetic acid solution. Then the mixture was shaken in an incubator shaker (New Brunswick, Innova 42/42R) at 100 rpm and 30 °C for 12 h. After addition of 25 g of CH pellets the chitosan solution was continuously shaken at 100 rpm and 30 °C for 24 h. The CHC pellets were placed on filters and rinsed with DI water until excess chitosan had been removed, then dried in the oven at 60 °C for 24 h. CHC was kept in a plastic bottle in a dry place and used for all experiments.

2.1.2 Pellets of biochar mixed with eggshell powder

Chicken eggshell was cleaned and crushed into powder. The coconut husk biochar powder was mixed with eggshell powder in a ratio of 1:1 (w/w), then the mixture was pelletized using corn flour as a binding agent followed the steps described above (2.1). Pelletized biochar mixed with eggshell powder (CHEG) was kept in a plastic bottle at a dry place and used for all experiments.

2.2 Characterization of biochar pellets

The C, H, N, and S contents of biochar pellets were analyzed using a Perkin Elmer 2400-II CHNS elemental analyzer. Oxygen content was obtained by calculation as 100 - %C - %H - %N - %S. The specific surface area was determined using Brunauer-Emmett-Teller (BET) nitrogen gas adsorption-desorption isotherms at 77 K with a surface analyzer (Autosorb-1, Quantachrome, BEL model, USA). The pore size distribution was measured from the nitrogen gas desorption using a Barrett-Joyner-Halenda analyzer. The iodine number was measured as a relative indicator of porosity following the ASTM D4607 method. Surface morphology images were analyzed by scanning electron microscopy (SEM, BRUKER). Fourier Transform Infrared (FTIR) spectroscopic analysis of biochar pellets indicated the functional groups on the surfaces as observed by a Thermo Scientific Nicolet 6700 spectrometer.

The ions released from the biochar pellets were determined after shaking 20 g L^{-1} of biochar in DI water at 120 rpm and 30 °C for 48 h. Then, the mixture was filtered through 0.45 μm membrane filters (Sartorius) before measuring Na^+, NH_4^+, K^+, Ca^{2+}, Mg^{2+}, Cl^-, NO_2^-, NO_3^-, PO_4^{3-} and SO_4^{2-} ions by Ion Chromatography (761 Compact IC, Metrohm; column Metrosep A Supp5–150/4.0 at flow rate of 0.7 mL min^{-1} for anion analysis and Metrosep C4–100/4.0 at flow rate of 0.9 mL min^{-1} for cation analysis).

The pH at zero-point of charge (pH_{zpc}) was analyzed using the pH drift method with a pH meter (WTW, pH 3210). Biochars (0.15 g) were placed in 125 mL flasks containing 50 mL of 0.01 N NaCl solution adjusted to different pH values of 1.0, 3.0, 5.0, 7.0, 9.0 and 11.0 using NaOH and HCl. The mixture was shaken at 120 rpm and 30 °C for 48 h, before measuring the final pH. The pH_{zpc} was where the initial pH equaled the final pH.

2.3 Batch experiments

Batch experiments were conducted to study the adsorption capacities of biochar pellets to remove nutrients in single solute and mixed solute systems. Stock solutions of nutrients at 1000 mg L^{-1} concentration were prepared using analytical grade ammonium chloride; NH_4Cl (Qrec), potassium nitrate; KNO_3 (Ajax Finechem), and potassium dihydrogen phosphate; KH_2PO_4 (Ajax Finechem). Then, the initial concentration of each nutrient was prepared by dilution of the stock solutions to 10 mg L^{-1} both in single and mixed solute solutions. All solutions were adjusted to pH 7 ± 0.5 using HCl and NaOH.

All biochar adsorbents (CH, CHC, and CHEG) were sterilized to prevent microbial activities in nutrient adsorption studies by using an autoclave (121 °C for 15 min) and then dried in an oven at 60 °C. The sterilized adsorbents were kept in sterilized and cleaned bottles in a dry place before being used for batch experiments. All experiments were done in triplicates.

To study the effect of the contact time of adsorption, 20 g L^{-1} of sterilized CH, CHC, and CHEG pellets were added into 50 mL centrifugal tubes containing each single and mixed solute solution. Control experiments were conducted using no adsorbate and no adsorbent. The mixtures were shaken and the water samples were collected periodically until reaching sorption equilibrium. The suspensions were filtered using sterilized 0.45 μm membranes (Satorius) before measuring the final pH, and NH_4^+, NO_3^-, and PO_4^{3-} concentrations by ion chromatography. The average aqueous concentration values were determined and the amount of adsorbate on the biochar, q_t (mg g^{-1}), was calculated using Eq. (1).

$$q_t = \frac{(C_i + C_b - C_e)V}{m} \tag{1}$$

C_i and C_e (mg L^{-1}) were the NH_4^+, NO_3^-, or PO_4^{3-} concentrations in solution at the initial and equilibrium time, respectively. V was the volume of the solution (L), and m the mass of biochar used (g). C_b (mg L^{-1}) was the concentration of NH_4^+, NO_3^-, and PO_4^{3-} released by biochar into DI water for the same condition of the nutrient adsorption study. The adsorption kinetics of nutrients in each single and mixed solute solutions were determined. The result was fitted with pseudo first order and pseudo second order kinetic models.

2.3.1 Adsorption isotherm study

Each single solute of NH_4^+, NO_3^-, and PO_4^{3-} solution was prepared at concentrations ranging from 10 to 100 mg L^{-1}. A mixed solution with NH_4^+, NO_3^-, and PO_4^{3-} each at concentrations ranging from 10 to 100 mg L^{-1} was also prepared. All solutions were adjusted to pH 7 ± 0.5 using HCl and NaOH. Sterilized CH and CHC pellets at a dosage of 20 g L^{-1} were used in this study. The solutions were shaken at 120 rpm and 30 °C for 48 h. Then, the final pH and concentration of NH_4^+, NO_3^- and PO_4^{3-} was measured for the filtrates. All experiments were done in triplicates. The average values were calculated and fit with typically monolayer and multilayer adsorption isotherm models, which were Langmuir, Freundlich, Sips, Dubinin-Radushkevich (D-R), and BET models according to Eqs. (2)–(6), respectively.

$$\text{Langmuir;} \quad q_e = \frac{q_{max}K_L C_e}{1 + K_L C_e} \tag{2}$$

$$\text{Freundlich;} \quad q_e = K_f C_e^{1/n_f} \tag{3}$$

$$\text{Sips;} \quad q_e = \frac{q_{max}K_s C_e^{n_s}}{1 + K_s C_e^{n_s}} \tag{4}$$

$$\mathrm{D-R;} \quad q_e = q_{max}e^{-\beta\varepsilon^2} \tag{5}$$

$$\text{BET;} \quad q_e = \frac{q_{BET}K_1 C_e}{(1 - K_2 C_e)(1 - K_2 C_e + K_1 C_e)} \tag{6}$$

where, C_e is the equilibrium concentrations (mg L^{-1}) and q_e the amount of nutrient adsorbed (mg g^{-1}) at equilibrium, with q_{max} being the maximum capacity ($mg\,g^{-1}$). K_L is the Langmuir constant ($L\,mg^{-1}$), K_f ($mg^{1-1/nf}\,L^{1/nf}\,g^{-1}$) the Freundlich constant, and $1/n_f$ (dimensionless) the Freundlich exponent. K_s ($L^{ns}\,mg^{-ns}$) and n_s (dimensionless) are Sips constants. The ε value of the Dubinin-Radushkevich model can be calculated as $\varepsilon = RT\ln(1+1/C)$, where R is a constant ($8.31\,J\,mol^{-1}\,K^{-1}$) and T is the temperature (K). C is a dimensionless concentration ratio $C_{e,molar}/C°$, where $C°$ is the standard state of the solute in aqueous solution equal to 1 M and $C_{e,molar}$ is the equilibrium concentration in units of M [20]. β is the Dubinin-Radushkevich constant ($mol^2\,J^{-2}$). K_1 and K_2 value are BET constants ($L\,mg^{-1}$).

2.3.2 Effect of initial pH

To study the effect of initial pH, each of the sterilized adsorbents at a dosage of $20\,g\,L^{-1}$ was placed into 50 mL centrifuge tubes containing a single or mixed solute solution with different initial pH values of 3, 5, 7, 9, and 11 (initial concentration of $10\,mg\,L^{-1}$). The mixtures were shaken for 48 h at 120 rpm and 30 °C. Then, the filtrates were used to determine the final pH and concentrations of NH_4^+, NO_3^- and PO_4^{3-}.

2.3.3 Effect of temperature

To study the effect of temperature, the dosage of each biochar was prepared as above. The initial concentration of single solute solution was 10–100 $mg\,L^{-1}$ (initial pH of 7). The mixtures were shaken for 48 h at 120 rpm at 25, 30, and 40 °C. The filtrates were collected to determine the concentration of NH_4^+, NO_3^-, and PO_4^{3-}.

The Gibbs free energy of adsorption (ΔG) is given by Eq. (7), The relationship of ΔG to the change of enthalpy (ΔH) and entropy (ΔS) of adsorption can be expressed as Eq. (8).

$$\Delta G = -RT\ln K_a \tag{7}$$

$$\ln K_a = \frac{\Delta S}{R} - \frac{\Delta H}{RT} \tag{8}$$

where the K_a is the dimensionless thermodynamic equilibrium constant [21, 22] and T is the temperature (K). Then, K_a can be estimated from the Langmuir isotherm as $K_a = (K_{L,molar}/\gamma_e) \times C_s$, which $K_{L,molar}$ is the Langmuir constant in units of M^{-1}, C_s is the standard reference solute concentration in aqueous solution, which is equal to 1 M, and γ_e is activity coefficient at adsorption equilibrium. γ_e is a function of the ionic strength (I_e) of the aqueous solution which depends on the concentration and the charge carried by the dissolved ions (z) according to log $\gamma_e = -Az^2I_e^{1/2}$ [21]. For neutral adsorbates or adsorbates with weak charges $\gamma_e \to 1$ [21]. In our experiments the γ_e value was calculated to be in the range of 0.75–0.98, and therefore K_a was approximated by $K_a = K_{L,\,molar} \times C_s$. The change of enthalpy (ΔH) and entropy (ΔS) can then be determined by the slope and intercept of the plot of $\ln K_a$ versus $1/T$.

2.3.4 Effect of surface water on nutrient adsorption

Surface water from the Khwang canal in a residential area of Bangkok, Thailand, was collected and sterilized in an autoclave (121 °C for 15 min). Each of the adsorbents at $20\,g\,L^{-1}$ was placed in 50 mL centrifugal tubes containing sterilized surface water. The control was using surface water without biochar addition. The mixtures were shaken at 120 ppm and 30 °C for equilibrium time 48 h (same condition as 2.3.1–2.3.2). The filtrates were used to measure the final pH and concentrations of NH_4^+, NO_3^-, and PO_4^{3-}. The nutrient removal efficiency of different biochar samples was calculated as per Eq. (9). C_i and C_e ($mg\,L^{-1}$) were the initial concentrations (NH_4^+, NO_3^-, and PO_4^{3-}) of sterilized surface water and equilibrium concentration after adsorption.

$$R\ (\%) = \frac{(C_i - C_e)}{C_i} \times 100 \tag{9}$$

3 Results and discussion

3.1 Characteristics of biochar and modified pellets

The properties of CH, CHC, and CHEG are compared in Table 1, which shows that the surfaces modification of biochar enhances the properties of the CH pellets. The iodine number of CHC was higher than that of CHEG and CH pellets, which corresponded to the trend for the BET surfaces. The low BET surface area of CH

Table 1 Properties of biochar pellets

Parameter	Unit	CH	CHC	CHEG
Iodine number	$mg\,g^{-1}$	123	187	150
BET	$m^2\,g^{-1}$	1.6	2.4	2.0
Total pore volume	$cm^3\,g^{-1}$	0.0025	0.0044	0.0016
Mean pore diameter	nm	6.3	7.5	3.3
pH_{DI}		7.21	6.11	8.10
pH_{ZPC}		7.10	6.10	7.58
Element				
C	%	68.5	63.3	31.9
H	%	3.5	3.1	1.9
O	%	27.8	27.2	65.2
N	%	0.06	6.3	0.60
S	%	0.15	0.04	0.01
H/C		0.08	0.05	0.06
O/C		0.14	0.43	2.06

was due to the high mineral content of alkaline biochar that can block access to the micropores [23]. Modification of CH biochar gave more potential for adsorption. The mean pore diameter of CH, CHC, and CHEG indicated mesopores with diameters of 2–50 nm. The mean pore diameter was CHC (7.5 nm) > CH (6.3 nm) > CHEG (3.3 nm). Eggshell powder might have blocked the pores, decreasing total pore volume and diameter. The pH of CH, CHC, and CHEG in DI water (pH_{DI}) was 7.21, 6.10, and 8.10, respectively. CHEG was moderately alkaline from the CaO and $CaCO_3$ in eggshell powder, since raw eggshell consists of 98.5% CaO [24]. CHC was weakly acidic due to the acetic acid used for chitosan coating. The pH values in aqueous solution of all adsorbents are greater than the pH_{zpc}, thus the adsorbent surfaces exhibit a net negative charge.

The atomic ratios of H/C and O/C indicate the aromaticity and polarity of biochar, respectively. In this study, the order of aromaticity was CH > CHEG > CHC, and the order of polarity was CHEG > CHC > CH. The higher polarity was caused by more oxygen-containing functional groups and surface hydrophilicity which improves the removal of inorganics [25]. The O/C ratio of CHEG had a 2-time increase compared with the original CH pellet (Table 1), indicating that CHEG had more oxygen-containing groups which promote the adsorption potential.

Biochar has functional groups on the carbonaceous surface such as hydroxylic, carboxylic, or phenolic moieties [26]. FTIR spectra of CH, CHEG, CHC, chitosan powder, and eggshell powder are shown in Fig. 2. The approximate peak at 3400 cm^{-1} was ascribed to -OH groups and -NH stretching vibrations [15]. The band at 2900 cm^{-1} was attributed to O-H and aliphatic C-H stretching, which indicated hemicellulose and cellulose structures [12]. CH, CHC, and CHEG showed a peak at 1740 cm^{-1} ascribed to C=O stretching. CHC had an acidic surface (pH = 6.1) as indicated by acidic functional group peaks of 1740 and 1370 cm^{-1}, representing carboxylic and phenolic groups [19, 25]. The peak at 1585 and 1215 cm^{-1} in CHC and chitosan (Fig. 2a) showed that CHC had chitosan coated on the surface, indicating the amine group. The sharp peaks of 712, 872, and 1400 cm^{-1} in eggshell and CHEG (Fig. 2b) were ascribed to Ca-O bonding, C-O stretching and C-H bonding, respectively, with the presence of CaO and $CaCO_3$ [7, 12].

SEM images show the morphologies of CH, CHC, and CHEG biochar in Fig. 3. Chitosan coating might be covering some surface area of CHC (Fig. 3b) which by and large retained the original biochar surface features. The CH SEM image also resembled that of CHEG. CHEG contained eggshell powder, and some eggshell fragments are indicated in Fig. 3c.

Inorganic components in biochar are dependent on the feed stocks. Figure 4 shows the concentration of anions and cations released from biochar into DI water. CH released ion concentrations greater than CHEG and CHC. The average total ion concentrations from CH, CHC, and CHEG were 52.6, 7.2 and 20.1 mg g^{-1}, respectively. High alkaline mineral contents of biochar may block biochar pores which was confirmed by low BET surface values. The order of ions released from CH was $Cl^- > K^+ > Na^+ > PO_4^{3-} > SO_4^{2-} > Ca^{2+} > NO_3^- > Mg^{2+} > NH_4^+ = NO_2^-$. According to Khawkomol et al. [19] the content of the metal components of coconut husk biochar was K > Cl > Na > Ca > Mg > P. The ions released from biochar could compete with nutrients for adsorption sites. Hence, these anions and cations may affect the nutrient adsorption.

3.2 Nutrient sorption and kinetic

The adsorption kinetics of NH_4^+, NO_3^-, and PO_4^{3-} in single and mixed solute solutions were investigated. The mixed solution system is more similar to actual water and wastewater systems, which consist of various ions including counter ions (Cl^- and K^+). The various ions in water or wastewater play an important role as competitors with the nutrients NH_4^+, NO_3^-, and PO_4^{3-} for adsorption sites and consequently decrease the adsorption efficiency for the individual ions by biochar [9]. An initial concentration of 10 mg L^{-1} with initial pH of 7 was used in this study due to the existence of nutrients at these typical concentration levels in surface water. The result showed that, contrary to the initial expectation, NH_4^+, NO_3^-, and PO_4^{3-} adsorption in single solute solution was less than for mixed solute solution (Fig. 5).

The adsorption kinetics of NH_4^+ in single and mixed solute solutions of CH, CHC, and CHEG are shown in Fig. 5a-b. CHC achieved sorption equilibrium within 4 h which was shorter than for CH (8 h) and CHEG (16 h) in single solute solutions. The equilibration times of NH_4^+ adsorption in mixed solute solution was longer than in single solute solution and required 8, 16, and 48 h for CHEG, CHC, and CH, respectively. However, the sorption capacity of NH_4^+ in mixed solute solution was higher than in single solute solution. CH, CHC, and CHEG had oxygen-containing functional groups on their surface which enhanced the NH_4^+ adsorption. The magnesium component of CH, CHC, and CHEG facilitated greater NH_4^+ adsorption. Mg^{2+} can be precipitated with NH_4^+ and PO_4^{3-} as $NH_4MgPO_4{\cdot}6H_2O$ or struvite on the biochar surface, which indicated another mechanism of NH_4^+ removal [5, 23] that would only occur in the mixed solute solution. The K_{sp} value of struvite is 12.6 [10]. The range of NH_4^+ sorption capacity of CH, CHC, and CHC in mixed solute solution was 0.6–1.7 mg g^{-1} and the

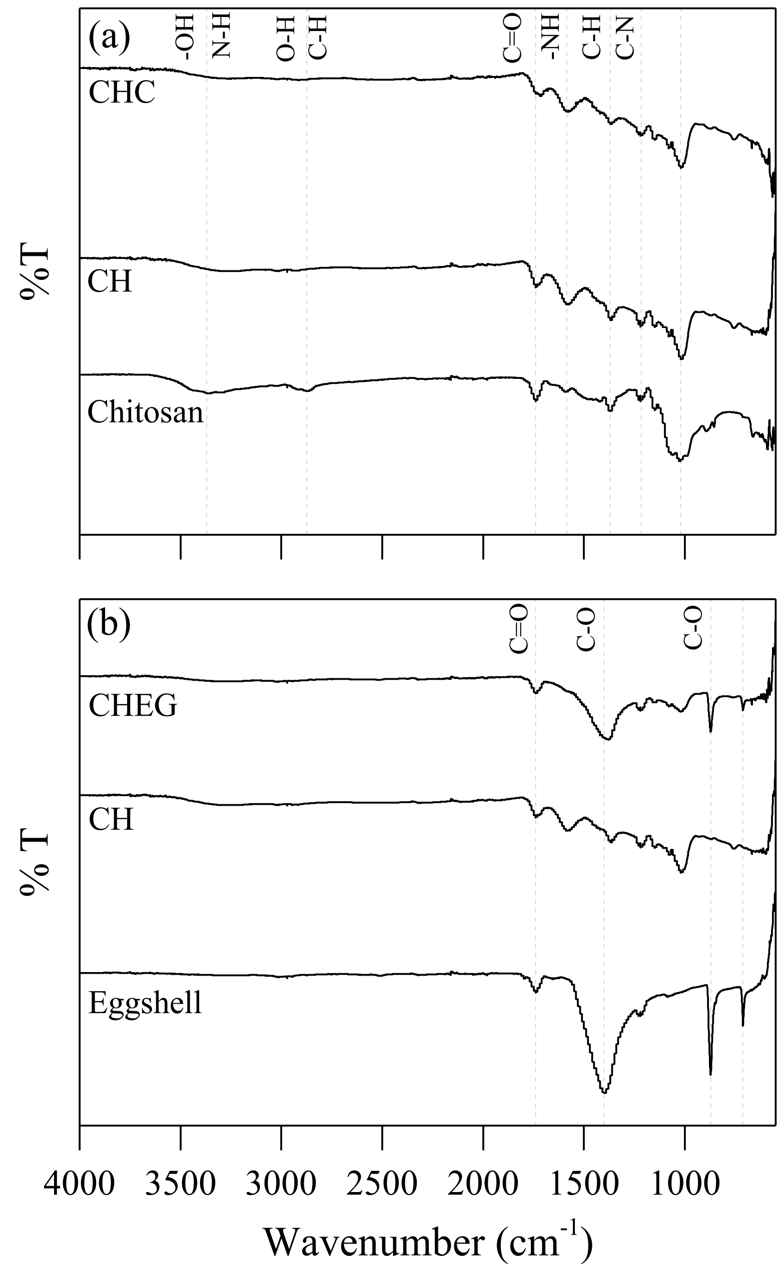

Fig. 2 FTIR spectra of biochar (**a**) CHC peaks compared with CH and chitosan powder, (**b**) CHEG peaks compared with CH and eggshell powder

percentage of NH_4^+ removal after 48 h ranged from 94 to greater than 99.9%.

The equilibration time of NO_3^- adsorption from a single solute solution by CHC (4 h) was shorter than for CH and CHEG (16 h), while for mixed solute solutions, the equilibration time of CHEG (6 h) was shorter than CH (16 h) and CHC (24 h). The order of equilibration time for NO_3^- adsorption in single and mixed solute solution was CHC > CHEG > CH. The surface modification by chitosan provided the positive charges of R-NH_3^+, consequently enhancing the attraction of NO_3^- towards CHC to form electrostatic R-NH_3^+-NO_3^- bonds. Furthermore, calcium in biochar and NO_3^- in the solution can form Ca $(NO_3)_2$ solid precipitates on biochar surfaces [12]. Although the biochar typically already contains Ca^{2+}, CHEG showed NO_3^- sorption better than CH (Fig. 5c-d). This result showed how Ca^{2+} from eggshell powder can promote NO_3^- removal. The sorption

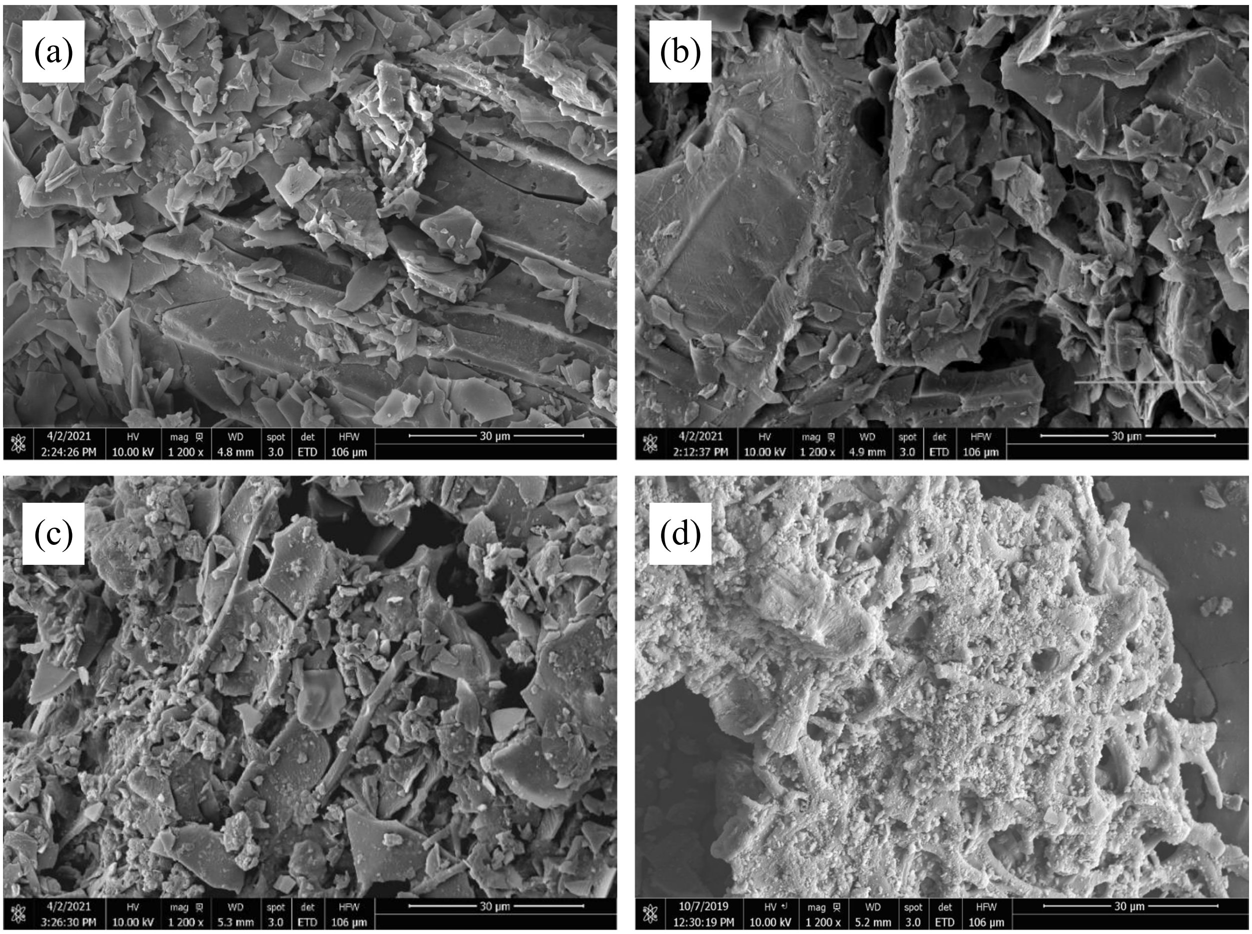

Fig. 3 SEM image on biochar surface of (**a**) CH, (**b**) CHC, (**c**) CHEG, and (**d**) eggshell powder

capacities of NO_3^- on CH, CHC, and CHEG ranged from 0.2–0.8 mg g^{-1} and the percentage of NO_3^- removal in mixed solute solution after 48 h was 47–100%.

The initial PO_4^{3-} concentration was 10 mg L^{-1}, but the CH, CHC, and CHEG also released PO_4^{3-} at 1.9, 0.5, and 0.3 mg g^{-1}, respectively into DI water. Thus, low adsorption capacities of all adsorbents were observed in single solute solution. Zhang et al. [9] also reported low PO_4^{3-} adsorption at low initial PO_4^{3-} concentration. At high concentration, steep gradients between biochar and the bulk solution result in better filling of reactive adsorption sites [27]. CH, CHC, and CHEG effectively adsorbed PO_4^{3-} from the mixed solute solution.

The pseudo first order and pseudo second order kinetic models were used to fit the adsorption data. The calculated kinetic parameters are given in Table 2. The correlation coefficient (R^2) for pseudo first order and pseudo second order model fits of NH_4^+, NO_3^-, and PO_4^{3-} adsorption data were similar. For NH_4^+, NO_3^-, and PO_4^{3-} adsorption on CH, CHC, and CHEG from single and mixed solute solutions the R^2 value was more than 0.9 except for the NO_3^- adsorption on CH in single solute solution with an R^2 value of 0.83. NO_3^- adsorption on CHC was well fit by the pseudo second order model in single and mixed solute solutions, while CH and CHEG data were best fit by the pseudo first order model. Based on R^2 values, the pseudo second order model fitted better than the pseudo first order model for PO_4^{3-} adsorption from mixed solute solution. Biochar pellets have heterogeneous surfaces with the proposed mechanism for PO_4^{3-} being that it is not adsorbed directly onto the biochar surface [28]. On the other hand, PO_4^{3-} could precipitate with metal ions (Ca^{2+} and Mg^{2+}) out of solution and onto biochar surfaces [29]. However, the PO_4^{3-} adsorption kinetics of CH, CHC, and CHEG in single solute solution could not be determined in this study due to the strong compounding effect of PO_4^{3-} released from biochar.

The rate of PO_4^{3-} adsorption rates onto CH was highest, followed by NO_3^- and NH_4^+, respectively, with k

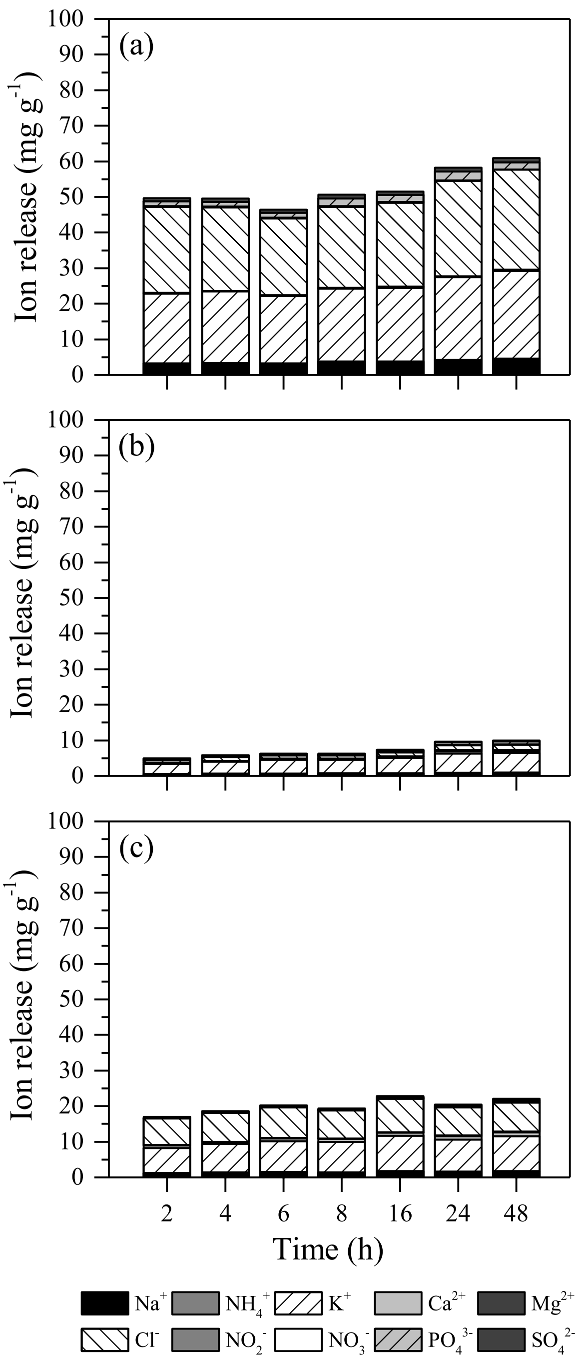

Fig. 4 Biochar at 20 g L^{-1} in DI water (**a**) CH, (**b**) CHC, and (**c**) CHEG, released different amounts of anions and cations after 2–48 h shaking at 120 rpm and temperature of 30 °C

values in the order of $PO_4^{3-} > NO_3^- > NH_4^+$ since the surface charge of CH was positive. CHC had a negative surface charge and hence electrostatic attraction can describe the NH_4^+ adsorption mechanism. The order of nutrient adsorption rates by CHC from mixed solute solution was NH_4^+ followed by PO_4^{3-} and NO_3^-, respectively (k of $NH_4^+ > PO_4^{3-} > NO_3^-$). The order of nutrient adsorption rates by CHEG was NH_4^+ followed by NO_3^- and PO_4^{3-}, respectively (k of $NH_4^+ > NO_3^- > PO_4^{3-}$).

3.3 Nutrient sorption isotherm

The NH_4^+, NO_3^-, and PO_4^{3-} adsorption capacities increased in a nonlinear way as the initial concentration increased both in single and mixed solute solutions (Fig. 6). Table 3 shows the adsorption parameters of each adsorbent using various adsorption isotherm models. The NH_4^+ adsorption capacities for the investigated concentrations were in the ranges of 0.2–2.2, 0.07–1.3 and 0.3–2.2 mg g^{-1} for CH, CHC, and CHEG, respectively (Fig. 6a). Nitrate adsorption capacities in single and mixed solute solutions of CH, CHC, and CHEG were in the ranges of 0.01–1.6, 0.2–1.4, and 0.2–3.5 mg g^{-1}, respectively. It was found that PO_4^{3-} was released from adsorbents if the initial PO_4^{3-} concentration was lower than 10 mg L^{-1} (Fig. 6c). The amount of PO_4^{3-} adsorbed increased as the initial PO_4^{3-} concentration increased, while the amount of PO_4^{3-} released from biochar would remain the same [9]. PO_4^{3-} adsorption on biochar increased with high initial concentration possibly due to higher concentration gradients, when PO_4^{3-} is better at filling active sites [27].

The equilibrium isotherms could be classified as S or L curves (Fig. 6). Ammonium adsorption on CH and CHEG in single and mixed solute solution was classified as L curves (type I) with a plateau that represented the maximum adsorption capacity as predicted by the Langmuir model. The curve of NH_4^+ adsorption on CHC (Fig. 6a) was classified as S curve (type VI) which represented a shorter plateau. This indicated that the solutes interacted with each other on the biochar surface resulting in multilayer adsorption [30]. A similar trend was observed for NO_3^- adsorption as single solute on CH (Fig. 6b). NO_3^- adsorption on CHC reached the maximum capacity of 1.6 and 1.3 mg g^{-1} for the single and mixed solute solution, respectively. NO_3^- in mixed solution also reached a maximum capacity for CHEG (0.9 mg g^{-1}). However, PO_4^{3-} adsorption on CH was described by a type III (concave upward curve) adsorption isotherm, meaning that the adsorbate–adsorbate interaction was more significant compared to adsorbate–sorbent interactions [31]. Furthermore, PO_4^{3-} adsorption on CHC and CHEG from single solute solution was described by a type V isotherm which is similar to type III, with adsorbate–adsorbate interactions being dominant, and filling of mesopores could have occurred [31].

The Langmuir model indicates monolayer adsorption on a homogenous surface, while the Freundlich

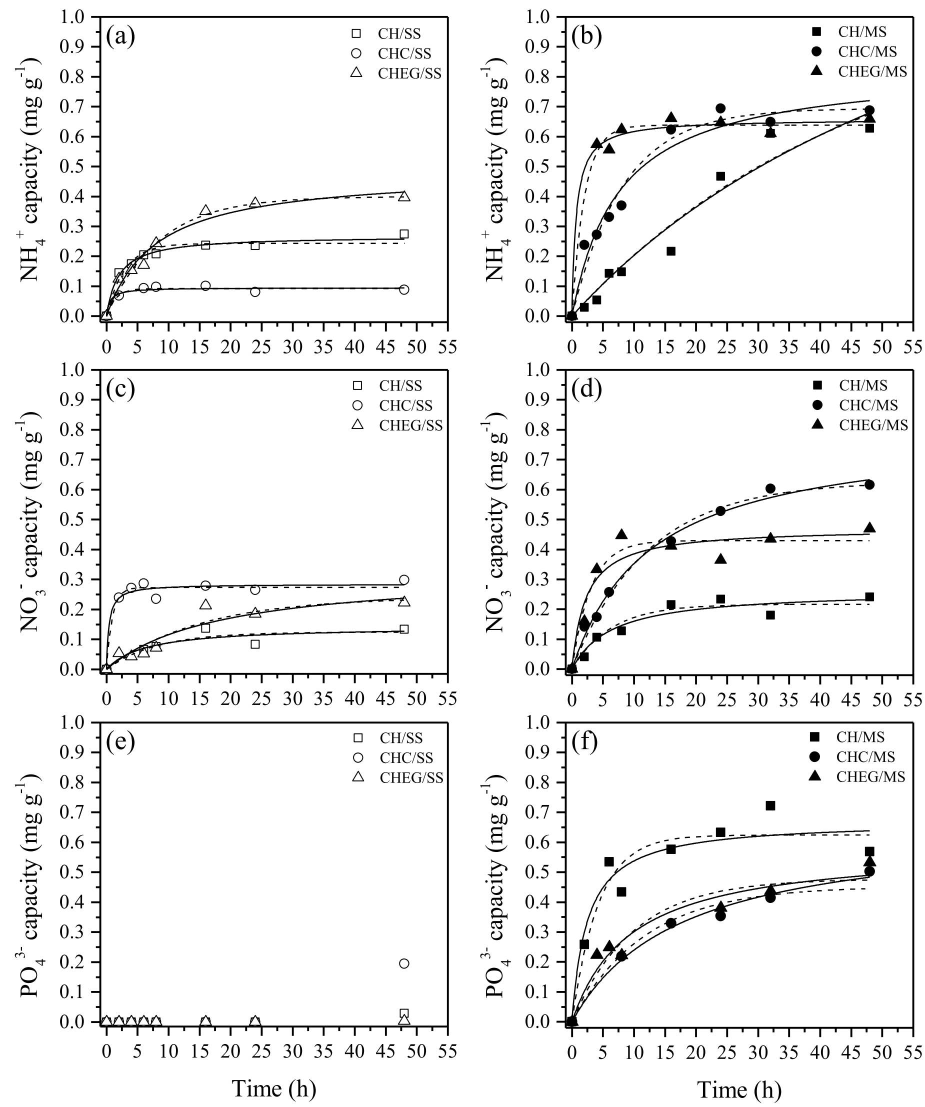

Fig. 5 Nutrient adsorption by 20 g L^{-1} of CH, CHC, and CHEG; adsorption of (**a**) NH_4^+ in single solute solution (SS); (**b**) NH_4^+ in mixed solute solution (MS); (**c**) NO_3^- in SS; (**d**) NO_3^- in MS; (**e**) PO_4^{3-} in SS; (**f**) PO_4^{3-} in MS; dashed line = fitted with pseudo first order kinetics model and solid line = fitted with pseudo second order kinetics model

isotherm indicates nonideal adsorption on heterogeneous surfaces and multilayer adsorption [32]. Freundlich isotherms best described the sorption of NH_4^+, NO_3^-, and PO_4^{3-} by CH, CHC, and CHEG, having high correlation coefficients with the data ($R^2 > 0.81$). Biochar has a heterogeneous surface due to the carbonized and non-carbonized phases of biochar generally representing different adsorption mechanisms [8]. The $1/n_f$ value indicates surface heterogeneity. The $1/n_f$ values of NH_4^+ sorbed by CH and CHEG in single and mixed solute solution were lower than 1 ($0 < 1/n_f < 1$) which implies heterogeneous surfaces favorable to adsorb NH_4^+. CHC in mixed solute solution showed unfavorable adsorption of NH_4^+ ($1/n_f > 1$), as the functional group of R-NH_3^+ could repulse the NH_4^+ ions in solution. The $1/n_f$ value of NO_3^- adsorption on CH, CHC, and CHEG was lower than 1 except for CH in single solute solution ($1/n_f > 1$). The CH, CHC, and CHEG was unfavorable to adsorb PO_4^{3-} in single solute solution ($1/n_f > 1$) while CHC and CHEG were favorable to adsorb PO_4^{3-} in mixed solute solution ($1/n_f < 1$). It was reported that PO_4^{3-} adsorption is not by direct interaction with the carbon surfaces but by precipitation with Ca^{2+} [29]. Eggshell has high calcium content which could precipitate with PO_4^{3-} in CHEG and PO_4^{3-} could also be attracted by chitosan surfaces (CHC). However, based on other research, biochar

Table 2 Parameters of pseudo first and second order kinetic models for nutrients adsorption from single and mixed solute solution

Model			Pseudo first order			Pseudo second order		
Parameter			q_e (mg g^{-1})	k_1 (h^{-1})	R^2	q_e (mg g^{-1})	k_2 (g mg^{-1} h^{-1})	R^2
NH_4^+	Single	CH	0.24	0.35	0.958	0.27	1.9	0.988
		CHC	0.09	0.71	0.964	0.09	19	0.944
		CHEG	0.40	0.12	0.980	0.48	0.26	0.974
	Mixed	CH	1.02	0.020	0.949	1.78	0.01	0.947
		CHC	0.69	0.12	0.963	0.84	0.16	0.958
		CHEG	0.64	0.49	0.984	0.66	2.2	0.987
NO_3^-	Single	CH	0.12	0.14	0.830	0.14	1.1	0.830
		CHC	0.27	1.06	0.965	0.28	8.9	0.966
		CHEG	0.24	0.07	0.900	0.33	0.16	0.866
	Mixed	CH	0.22	0.16	0.914	0.27	0.59	0.904
		CHC	0.63	0.08	0.990	0.80	0.10	0.992
		CHEG	0.43	0.33	0.942	0.47	0.94	0.916
PO_4^{3-}	Mixed	CH	0.62	0.23	0.928	0.67	0.60	0.930
		CHC	0.45	0.09	0.966	0.66	0.080	0.989
		CHEG	0.48	0.10	0.924	0.59	0.18	0.953

is an effective adsorbent for PO_4^{3-} even without modification [9, 13].

Furthermore, the D-R adsorption isotherm is applicable for heterogeneous surfaces, describing the physisorption and chemisorption of adsorbates on biochar by calculation of the mean free energy ($E = (1/2\beta)^{1/2}$) [30, 33]. An E value less than 8 kJ mol^{-1} indicates that adsorption is predominantly by physical interactions, while E value higher than 8 kJ mol^{-1} signifies chemisorption. It was found the mechanism of NH_4^+ and NO_3^- adsorption on CH and CHEG in single and mixed solutes indicated chemical adsorption. The E values were in the range of 8–16 kJ mol^{-1}. CHC showed physical interaction with NH_4^+ and chemical interaction with NO_3^-. PO_4^{3-} adsorption in this study was thus mainly physical interactions ($E < 8$ kJ mol^{-1}), i.e., pore filling or electrostatic attraction. The prediction of q_{max} values using the D-R isotherm was unreliable for PO_4^{3-} adsorption in this study (Table 3), due to the measured data not reaching the anticipated plateau in the curve (Fig. 6c). It should also be noted that the D-R isotherm might not always reliably distinguish between physical or chemical adsorption in complex solid/liquid adsorption systems and is mainly used for curve fitting and parameter value predictions [33].

The three-parameter Sips isotherm model is well suited to predict adsorption on heterogeneous surfaces and identify adsorption without adsorbate-adsorbate interactions as it combines the Langmuir and Freundlich isotherm models [34]. Adsorption then follows the Freundlich model at low initial concentration and the Langmuir model at high initial concentration. Therefore, the Sips model is used to describe monolayer adsorption. A n_s value of the Sips isotherm between 0 and 1 indicates heterogeneous surfaces while an n_s value close to 1 indicates more homogeneous surfaces [34]. Accordingly, CH, CHC, and CHEG had heterogeneous surfaces unfavorable for PO_4^{3-} adsorption both in single and mixed solute solution studies ($n_s >> 1$) except CHEG in mixed solute solution ($n_s = 1.0$).

The BET model can describe multilayer adsorption behavior [31, 34]. It has the same assumptions as the Langmuir model, but with multiple adsorption layers having different adsorption energy [31]. NH_4^+ and NO_3^- adsorption studies in single and mixed solute solution of CH, CHC, and CHEG indicated multiple layers of adsorption since the data were well fitted with the BET isotherm ($R^2 > 0.93$).

3.4 Effect of initial pH on adsorption

The initial pH of the solution affects the adsorption mechanism by determining the surface charge of an adsorbent. Figure 7 shows the NH_4^+, NO_3^-, and PO_4^{3-} sorption capacities for different initial pH values in single and mixed solute solution. The final pH of adsorption studies on CH, CHC, and CHEG in single solute solution ranged from 7.1–7.9, 4.7–7.4, and 7.3–9.1, respectively. The final pH on CH, CHC, and CHEG in mixed solute solution ranged from 6.7–7.9, 5.2–7.7, and 7.5–8.2, respectively.

The NH_4^+ adsorption capacity increased when the initial pH increased from 3 to 7. However, the NH_4^+

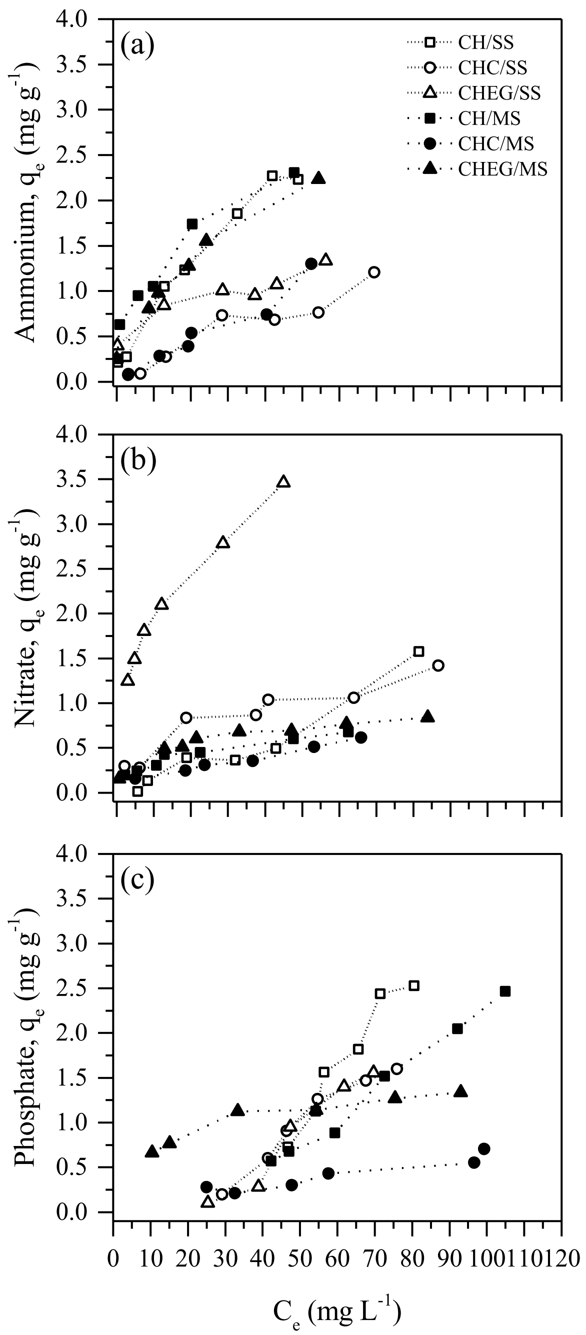

Fig. 6 Nutrient adsorption in single and mixed solute solutions at equilibrium time of 48 h; (**a**) NH_4^+, (**b**) NO_3^- and (**c**) PO_4^{3-} (SS = single solute, MS = mixed solute)

sorption capacity decreased when the initial pH value rose from 9 to 11. This result was confirmed by other researchers [10, 35, 36]. Biochar with high negative zeta potential facilitates NH_4^+ adsorption through electrostatic attraction, but when pH is increased to 10, the NH_4^+ cation would be transformed into NH_3 in the aqueous phase [37]. This study confirmed that the adsorption capacity decreased when pH increased towards 11 in closed batch systems which indicates ammonia stripping was not the mechanism for NH_4^+ removal, similar to the findings of Vu et al. [38]. The NH_4^+ adsorption by CH, CHC, and CHEG from mixed solute solution was better than for single solute solution. The highest NH_4^+ sorption capacities of CH, CHC, and CHEG were 0.41, 0.37, and 0.40 mg g^{-1}, respectively, in a single solute solution and they were 0.63, 0.69, and 0.66 mg g^{-1} in mixed solute solution at the initial pH in the range between 7 and 11. The high amount of H^+ in the lower pH range might compete with NH_4^+ for adsorption sites. At low pH electrostatic repulsion occurs between cations and the positive charge of the protonated biochar surfaces [8].

The NO_3^- adsorption on CH, CHC, and CHEG from mixed solute solution was higher than from single solute solution for initial pH 3–11 except for CHC and CHEG at initial pH 11. The highest NO_3^- sorption capacity of CH was found at initial pH 3, being 0.31 and 0.61 mg g^{-1} in single and mixed solute solution. At low pH, H^+ attachment to the biochar surface can attract NO_3^- by electrostatic charge and facilitate the removal of NO_3^- in solution. However, when the initial pH was acidic following HCl addition, the Cl^- concentration would have increased in the solution. Cl^- can compete with NO_3^- for the attractive sites on the adsorbent surface [12]. The highest NO_3^- sorption capacity of CHC was found at initial pH 5 and 7 of 0.52 and 0.62 mg g^{-1} in single and mixed solute solution, respectively. The highest NO_3^- sorption capacity of CHEG was found at initial pH 11 and 3 of 0.60 and 0.65 mg g^{-1} in single and mixed solute solution, respectively. At alkaline pH (pH = 11) the eggshell fragments in CHEG significantly adsorbed NO_3^- in solution.

Depending on the solution pH, phosphate exists in aqueous solution in the form of H_3PO_4, $H_2PO_4^-$, HPO_4^{2-} and PO_4^{3-}, where pK_1, pK_2, pK_3 values are 2.13, 7.20, and 12.33 [16]. The PO_4^{3-} adsorption of all adsorbents in mixed solute solution increased compared with single solute solution at initial pH of 3–11. An initial pH of 3 represented the highest PO_4^{3-} sorption capacity of CH, CHC, and CHEG in mixed solute solution. CH had the highest adsorption capacity of 1.9 mg g^{-1} followed by CHC (1.1 mg g^{-1}) and CHEG (0.9 mg g^{-1}). The H^+ ions at acidic conditions can protonate the active sites (positive charge) of the biochar surface to adsorb PO_4^{3-}. The R-NH_2 amino functional group of chitosan on CHC is protonated (R-NH_3^+) when pH is low which enhances the PO_4^{3-} adsorption by electrostatic attraction [15]. However, the highest PO_4^{3-} sorption capacity in single solute solution of CH, CHC, and CHEG was found at an initial pH of 11. It was 0.44, 0.37, and 0.18 mg g^{-1} of CH,

Table 3 Various isotherm parameters for nutrient adsorption onto biochar pellets in the single and mixed solute solutions

Model			**Langmuir**			**Freundlich**			**Sips**				**Dubinin-Radushkevich**				**BET**			
Parameter			K_L (L mg^{-1})	q_{max} (mg g^{-1})	R^2	K_F (mg$^{1-1/nf}$ L$^{1/nf}$ g^{-1})	$1/n_f$	R^2	q_{max} (mg g^{-1})	K_s (L^{ns} mg^{-ns})	n_s	R^2	q_{max} (mg g^{-1})	B (mol^2 J^{-2})	E (kJ mol^{-1})	R^2	q_{BET} (mg g^{-1})	K_1 (L mg^{-1})	K_2 (L mg^{-1})	R^2
NH_4^+	Single	CH	0.024	4.27	0.986	2.1×10^{-1}	0.63	0.984	5.28	2.3×10^{-2}	0.91	0.987	11.89	7.35×10^{-9}	8.3	0.986	2.00	6.5×10^{-2}	6.0×10^{-3}	0.984
		CHC	0.006	3.59	0.923	3.4×10^{-2}	0.82	0.909	5.02	6.0×10^{-3}	0.92	0.924	4.87	8.30×10^{-9}	7.9	0.907	0.65	5.1×10^{-2}	7.0×10^{-3}	0.934
		CHEG	0.102	1.38	0.604	5.1×10^{-1}	0.21	0.882	5.66	9.9×10^{-2}	0.24	0.873	1.70	1.90×10^{-9}	16	0.873	0.74	6.9	8.0×10^{-3}	0.973
	Mixed	CH	0.076	2.88	0.891	5.2×10^{-1}	0.38	0.952	5.03	9.9×10^{-2}	0.54	0.943	5.86	4.29×10^{-9}	11	0.940	1.21	9.1×10^{-1}	1.0×10^{-2}	0.931
		CHC	0.009	3.41	0.905	1.9×10^{-2}	1.04	0.929	4.67	3.0×10^{-3}	1.21	0.934	18.25	1.26×10^{-8}	6.2	0.935	0.39	1.3×10^{-1}	1.3×10^{-2}	0.980
		CHEG	0.034	3.43	0.969	2.8×10^{-1}	0.52	0.964	5.89	3.2×10^{-2}	0.74	0.970	8.82	6.40×10^{-9}	8.8	0.970	2.33	5.6×10^{-2}	3.0×10^{-3}	0.970
NO_3^-	Single	CH	0.005	4.45	0.845	3.0×10^{-3}	1.43	0.949	5.67	1.0×10^{-3}	1.28	0.924	6.43	7.58×10^{-9}	8.1	0.852	0.37	6.2×10^{-2}	9.0×10^{-3}	0.983
		CHC	0.044	1.60	0.907	1.8×10^{-1}	0.45	0.917	1.52	3.9×10^{-2}	1.07	0.928	3.71	3.83×10^{-9}	11	0.929	0.97	1.3×10^{-1}	4.0×10^{-3}	0.938
		CHEG	0.125	3.80	0.949	8.4×10^{-1}	0.37	0.994	7.70	1.1×10^{-1}	0.52	0.990	10.60	3.46×10^{-9}	12	0.992	2.29	3.5×10^{-1}	8.0×10^{-3}	0.999
	Mixed	CH	0.081	0.76	0.930	1.4×10^{-1}	0.38	0.965	1.27	9.3×10^{-2}	0.59	0.967	2.06	3.74×10^{-9}	11	0.969	0.42	2.4×10^{-1}	7.0×10^{-3}	0.955
		CHC	0.013	1.28	0.927	3.9×10^{-2}	0.65	0.953	1.65	2.5×10^{-2}	0.71	0.932	4.21	6.66×10^{-9}	8.7	0.946	0.27	2.1×10^{-1}	9.0×10^{-3}	0.987
		CHEG	0.087	0.91	0.933	2.2×10^{-1}	0.30	0.978	1.73	1.3×10^{-1}	0.45	0.988	1.87	2.92×10^{-6}	0.4	0.988	0.58	5.1×10^{-1}	4.0×10^{-3}	0.973
PO_4^{3-}	Single	CH	NA	NA	NA	5.1×10^{-4}	1.96	0.892	5.08	1.6×10^{-6}	3.06	0.940	2270.88	2.12×10^{-8}	4.8	0.917	41.03	3.2×10^{-4}	5.0×10^{-3}	0.890
		CHC	NA	NA	NA	2.0×10^{-3}	1.51	0.896	2.90	5.8×10^{-5}	2.32	0.952	299.11	1.60×10^{-8}	5.6	0.924	35.80	3.6×10^{-4}	3.0×10^{-3}	0.895
		CHEG	NA	NA	NA	1.4×10^{-4}	2.20	0.900	4.99	6.3×10^{-6}	2.65	0.929	3503.18	2.32×10^{-8}	4.6	0.923	37.28	1.9×10^{-4}	6.0×10^{-3}	0.824
	Mixed	CH	0.001	14.83	0.846	1.1×10^{-2}	1.08	0.815	1.89	6.9×10^{-7}	3.53	0.940	59.28	1.19×10^{-8}	6.5	0.871	3.12	5.0×10^{-3}	2.0×10^{-3}	0.805
		CHC	0.001	6.91	0.921	1.2×10^{-2}	0.87	0.914	1.10	7.7×10^{-4}	1.63	0.925	14.21	1.04×10^{-8}	6.9	0.922	2.68	3.0×10^{-3}	8.1×10^{-4}	0.921
		CHEG	0.073	1.50	0.975	3.6×10^{-1}	0.30	0.934	1.50	7.4×10^{-2}	1.00	0.976	3.32	2.95×10^{-9}	13	0.957	1.42	8.2×10^{-2}	4.8×10^{-4}	0.976

NA means not applicable

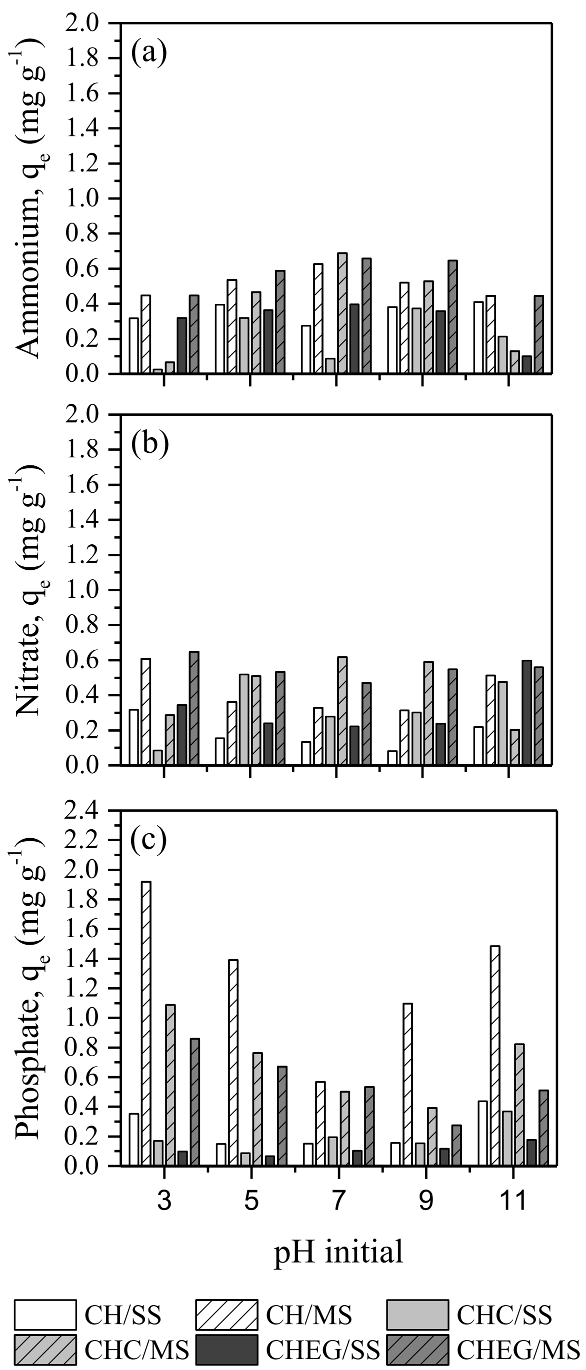

Fig. 7 Effect of different initial pH values on nutrient adsorption in single and mixed solute solutions; (**a**) NH_4^+ adsorption; (**b**) NO_3^- adsorption; (**c**) PO_4^{3-} adsorption (SS = single solute and MS = mixed solute)

CHC, and CHEG, respectively. When the solution pH was alkaline (pH 9–11), PO_4^{3-} could form stable complexes with Ca^{2+} and Mg^{2+} cations when the presence of anions such as Cl^-, NO_3^- and SO_4^{2-} in the solution were not a substantial competition [14]. HPO_4^{2-} and PO_4^{3-} are the predominant species at pH solution of 7–9, and these species may also form complexes with Ca^{2+} and Mg^{2+} but precipitation of phosphate and Ca^{2+} is unlikely to occur at a pH of 6.5 [29].

3.5 Effect of temperature

Biochar strongly affected PO_4^{3-} the adsorption because it released PO_4^{3-} into the solution especially at low initial concentration, and the measured isotherm data did not reach a plateau at high concentration and was therefore poorly fitted by the Langmuir adsorption model. Thus, NH_4^+ and NO_3^- were selected to investigate thermodynamics in this study. The thermodynamic parameters of nutrient adsorption in single solute solution are shown in Table 4. The negative ΔG value of NH_4^+ and NO_3^- adsorption on CH, CHC, and CHEG indicated favorable and spontaneous processes. However, it is noted that the batch adsorption study was conducted in an incubator shaker, and the agitation of the shaker might have enhanced nutrient adsorption. Moreover, the trend of more negative ΔG value with increasing temperature for CH, CHC and CHEG means that nutrient adsorption improves at higher temperature. It suggests sufficient energy is available to transport ions into the inner biochar pores [10].

Depending on the biochar and solution, the results showed endothermic processes (positive ΔH values) of NH_4^+ and NO_3^- adsorption. Only NH_4^+ adsorption on CH showed exothermic processes. Furthermore, ΔH can indicate the interactions between the adsorbent and adsorbate. For physical adsorption, such as van der Waals interactions, ΔH is usually lower than 20 kJ mol^{-1} and from 20 to 80 kJ mol^{-1} it shows electrostatic interaction [30]. A ΔH value from 80 to 450 kJ mol^{-1} indicates chemical bonding [29]. Apart from CH, ΔH values were higher than 80 kJ mol^{-1}, indicating the bonding between adsorbate and biochar surface. For CH, NH_4^+ had a negative ΔH value, while for NO_3^- physisorption was indicated, i.e., van der Waals interactions (ΔH = 7.8 kJ mol^{-1}). CHC showed the highest ΔH value on NO_3^- adsorption of 246 kJ mol^{-1}. It means chemical bonding between chitosan (R-NH_2^+) and NO_3^- occurred. Moreover, the eggshell in CHEG can also react with NO_3^-. The positive values of ΔS showed randomness at the solid–liquid interface during adsorption, which is due to the presence of non-pyrolyzed biochar from the biochar production.

Based on the results from the thermodynamic analysis, CHC and CHEG can strongly adsorb NH_4^+ and NO_3^- in actual water and wastewater treatment applications as indicated by negative free energy and enthalpy values of the adsorption.

Table 4 Thermodynamic parameters of NH_4^+ and NO_3^- adsorption in single solute solution

Parameter	Temp.	lnK_a	ΔG (kJ mol^{-1})	ΔS (kJ K^{-1} mol^{-1})	ΔH (kJ mol^{-1})	R^2
NH_4^+						
CH	298	8.1	−20	−0.21	−81	0.486
	303	6.1	−15			
	313	6.3	−16			
CHC	298	3.1	−8	0.57	163	0.979
	303	4.7	−12			
	313	6.4	−17			
CHEG	298	7.6	−19	0.51	134	0.873
	303	7.5	−19			
	313	10.0	−26			
NO_3^-						
CH	298	6.5	−16	0.08	8	0.033
	303	5.7	−14			
	313	6.5	−17			
CHC	298	4.2	−10	0.87	246	0.832
	303	7.9	−20			
	313	9.4	−24			
CHEG	298	4.2	−10	0.75	209	0.573
	303	9.0	−22			
	313	8.9	−23			

3.6 Nutrient adsorption mechanisms

The original and modified biochar surfaces contain different characteristics, which consequently affected the adsorption capacity. It was found that nutrient adsorption capacity at equilibrium in mixed solute solution was greater than in single solute solution (Fig. 7). In contrast, Yin et al. [13] found adsorption of NH_4^+, NO_3^-, and PO_4^{3-} on soybean straw biochar in tri-solute solutions was decreased compared to single solute solutions. Different types of biochars have different physical and chemical properties that affect nutrient adsorption. The nutrient adsorption capacity of different adsorbents is summarized in Table 5. A diagram of nutrient adsorption mechanisms of CH, CHC, and CHEG in mixed solute solution is shown in Fig. 8. The ionic radius of NH_4^+, NO_3^-, and PO_4^{3-} was 0.148, 0.179, and 0.238 nm. The pore diameter of CH, CHC, and CHEG was 6.3, 7.5, and 3.3 nm, respectively (Table 1), which means that NH_4^+, NO_3^-, and PO_4^{3-} ions in solution can readily migrate into the pores of biochar. Although PO_4^{3-} can access the pores, the phosphate leaching from biochar is also significant, especially for CH. For PO_4^{3-} adsorption in the single solute study, the high concentration gradient brought about a net release of phosphate ions instead of adsorption (Fig. 5e). However, PO_4^{3-} might also be removed from solution by other mechanisms.

According to the FTIR spectra of biochar in this study (Fig. 2), there are oxygen containing groups including hydroxyl and carboxyl on biochar surfaces. These functional groups on the biochar can be protonated or deprotonated depending on the solution pH, as shown in Eq. (10). Fan et al. [10] reported that -O$^-$ was typically the dominant oxygen species on biochar surfaces.

$$\text{Biochar} \cdots O^- + H^+ \leftrightarrow \text{Biochar} \cdots OH + H^+ \leftrightarrow \text{Biochar} \cdots OH_2^+ \quad (10)$$

CH, CHC, and CHEG had a net negative charge on their surfaces at neutral pH ($pH_{solution} > pH_{zpc}$) which enabled strong interactions with NH_4^+ in solution following Eqs. (11)–(12). After biochar adsorbed NH_4^+ ions from the solution, it might itself attract anions in the solution according to Eqs. (13)–(14) to increase NO_3^- and PO_4^{3-} adsorption capacity. However, the electrostatic attraction between NH_4^+ ions on the biochar and the anionic nutrients in the solution can be interfered with by other anions such as Cl^-. Chloride and other anions generally compete with NO_3^- and PO_4^{3-} for the sorption sites on the biochar.

$$\text{Biochar} + NH_4^+ \rightarrow \text{Biochar} - NH_4^+ \quad (11)$$

$$\text{Biochar} \cdots OH + NH_4^+ \rightarrow \text{Biochar} \cdots ONH_4 + H^+ \quad (12)$$

$$\text{Biochar} - NH_4^+ + NO_3^- \rightarrow \text{Biochar} - NH_4^+ \cdots NO_3^- \quad (13)$$

Table 5 Comparison of the nutrient adsorption capacity of different adsorbents

Biochar/Adsorbent	Pyrolysis(°C)	Treatment		Solution	Adsorbate	Adsorption capacity ($mg\,g^{-1}$)	Ref.
		Pre-	Post-				
Giant reed straw	500	–	–	NH_4^+	NH_4^+	1.5	34
Corncob	400	–	–	NH_4^+	NH_4^+	2.5	37
Corncob	400	–	HNO_3	NH_4^+	NH_4^+	2.6	37
Rubber tyre	NA	–	–	NO_3^-	NO_3^-	16	22
Soybean	400	–	HCl	$NO_3^- + NO_2^-$	NO_3^-	8.6	38
Chitosan microspheres	–	–	–	NO_3^-	NO_3^-	32	15
Chitosan microspheres	–	–	–	PO_4^{3-}	PO_4^{3-}	34	15
Oak wood	600	–	–	PO_4^{3-}	PO_4^{3-}	3.6	26
Oak wood	250	–	–	PO_4^{3-}	PO_4^{3-}	27	26
Soybean straw	500	–	–	$NH_4^+ + NO_3^- + PO_4^{3-}$	NH_4^+	≈ 0.50	13
Soybean straw	500	–	–	$NH_4^+ + NO_3^- + PO_4^{3-}$	PO_4^{3-}	≈ 2.5	13
Soybean straw	500	$AlCl_3$	–	$NH_4^+ + NO_3^- + PO_4^{3-}$	NO_3^-	≈ 7.0	13
Coconut husk	400	–	–	$NH_4^+ + NO_3^- + PO_4^{3-}$	NH_4^+	5.0	This study
Coconut husk	400	–	chitosan	$NH_4^+ + NO_3^- + PO_4^{3-}$	NO_3^-	1.6	This study
Coconut husk	400	–	eggshell	$NH_4^+ + NO_3^- + PO_4^{3-}$	PO_4^{3-}	1.5	This study

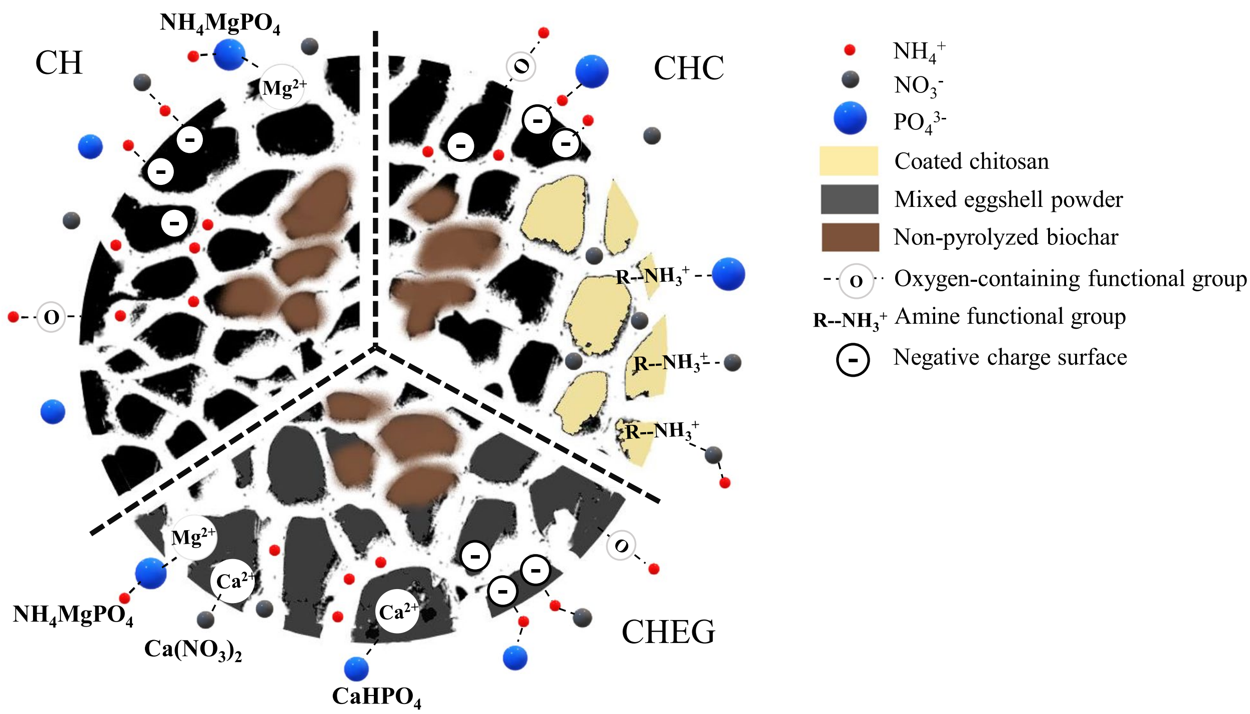

Fig. 8 Diagram of nutrient adsorption mechanisms on surfaces of biochar pellets in mixed solute solution

$$\text{Biochar} - NH_4^+ + PO_4^{3-} \rightarrow \text{Biochar} - NH_4^+ \cdots PO_4^{3-} \quad (14)$$

CHC surfaces have amino groups ($R\text{-}NH_3^+$) which could repulse the positive charges of NH_4^+, but it can adsorb NH_4^+ via other mechanism, such as pore filling and electrostatic attraction with the negative charges of non-chitosan coated areas (Eq. (12)). Struvite (NH_4MgPO_4) formation in solution could also explain the increased NH_4^+ and PO_4^{3-} removal in mixed solute solution (Eq. (15)).

$$NH_4^+ + Mg^{2+} + PO_4^{3-} + 6H_2O \rightarrow NH_4MgPO_4 \bullet 6H_2O\ (s) \quad (15)$$

Biochar has a net negative surface charge that can affect the anions adsorption but CH, CHC, and CHEG were nonetheless able to adsorb NO_3^- and PO_4^{3-} in mixed solution which some functional groups on their surfaces (Eqs. (16)–(18)).

$$\text{Biochar} \cdots OH^- + NO_3^- \left(\text{or } PO_4^{3-}\right) \rightarrow \text{Biochar} \cdots NO_3^- \left(\text{or } PO_4^{3-}\right) + OH^- \quad (16)$$

$$\text{Biochar} \cdots OH_2^+ + NO_3^- \left(\text{or } PO_4^{3-}\right) \rightarrow \text{Biochar} \cdots OH_2^+ \cdots NO_3^- \left(\text{or } PO_4^{3-}\right) \quad (17)$$

$$\text{Biochar} \cdots NH_3^+ + NO_3^- \left(\text{or } PO_4^{3-}\right) \rightarrow \text{Biochar} \cdots NH_3^+ \cdots NO_3^- \left(\text{or } PO_4^{3-}\right) \quad (18)$$

The Ca^{2+} and Mg^{2+} content in biochar could have facilitated precipitation or surface deposition as mechanisms for PO_4^{3-} adsorption in the form of $CaHPO_4$ and $MgHPO_4$.

3.7 Nutrient removal from surface water

The existence of various ions and other solutes in surface water could affect nutrient adsorption by competition for the surface adsorption sites. To avoid microbial activities during adsorption, surface water with high nutrient content from a canal in central Bangkok was sterilized. The average initial concentration of sterilized surface water was 10.7 mg NH_4^+ L^{-1}, 1.4 mg NO_3^- L^{-1} and 3.9 mg PO_4^{3-} L^{-1} with an initial pH = 7.9. It was found that the final pH after 48 h of CH, CHC, and CHEG adsorption was slightly decreased to 7.7, 7.2, and 7.7, respectively. CH, CHC, and CHEG at 20 g L^{-1} dosage removed NH_4^+ by 33, 24, and 37%, respectively (Fig. 9). NO_3^- could not be removed by CH and CHEG due to the strong repulsion effect of the negatively charged surfaces. However, the efficiency of NO_3^- removal by CHC from sterilized surface water was 25%. Coexisting ions in surface water will affect biochar adsorption. For example, NO_2^- and NO_3^- ions could compete on the biochar surface due to NO_2^- adsorption capacity being higher than NO_3^- in binary (NO_2^- + NO_3^-) solution [39]. PO_4^{3-} removal could not be achieved with CH, while CHC and CHEG effectively removed PO_4^{3-} by 66 and 58%, respectively. The R-NH_3^+ functional group on CHC was thus confirmed to facilitate NO_3^- and PO_4^{3-} removal by electrostatic attraction in solution. In addition, calcium is a main component of CHEG, and the precipitation with Ca^{2+} out of solution is likely the main mechanism of PO_4^{3-} removal, which can explain greater PO_4^{3-} than NO_3^- removal. Overall, CHC was the best adsorbent for simultaneously treating NH_4^+, NO_3^-, and PO_4^{3-} pollution in surface water. This removal of nutrients in this study was by the adsorption process only without biodegradation and biosorption. Therefore, the influence of microbial attachment to biochar surfaces should be investigated in further studies to optimize nutrient removal.

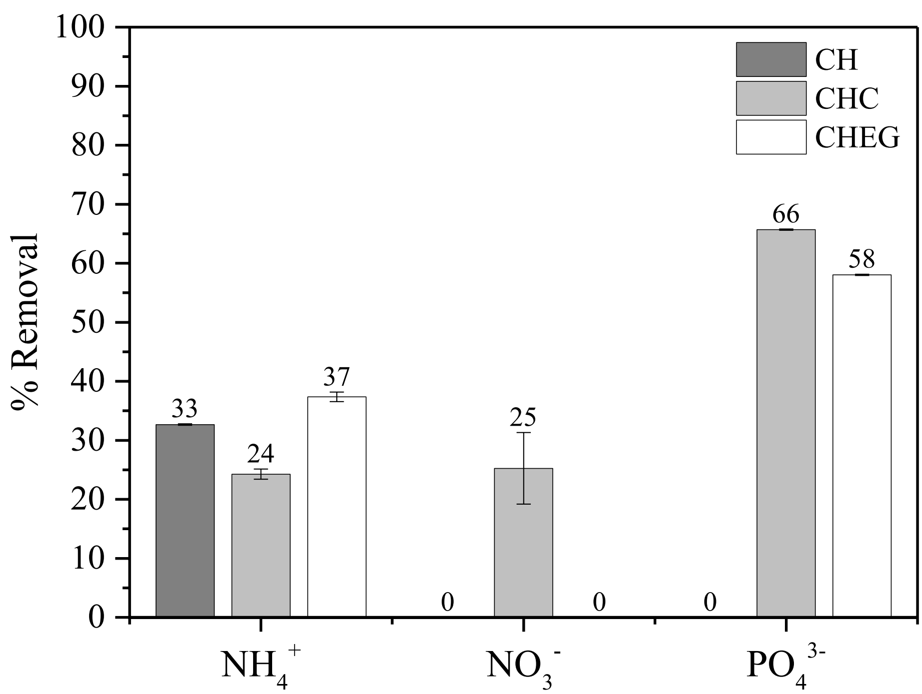

Fig. 9 The percentage of NH_4^+, NO_3^-, and PO_4^{3-} removal by 20 g L^{-1} of CH, CHC, and CHEG in sterilized surface water at time 48 h

4 Conclusions

The initial pH of solution strongly affected the nutrient (NH_4^+, NO_3^- and PO_4^{3-}) adsorption, affecting charge of surfaces and functional groups of the biochar. The adsorption mechanism of nutrient adsorption could be well described with the Sips isotherm model, which at low initial concentration follows the Freundlich model and at high initial concentration follows the Langmuir model. The nutrient adsorption mechanisms showed both physisorption and chemisorption. PO_4^{3-} adsorption was predominantly physical interaction, including pore-filling and electrostatic attraction by charge and functional group on biochar surfaces. Besides, chemical bonding can happen in NH_4^+ and NO_3^- adsorption on biochar surface.

CH, CHC, and CHEG were able to adsorb NH_4^+ in surface water which was present at of low initial concentration. The surface modification of biochar as CHC and CHEG enhanced the adsorption of NO_3^- and PO_4^{3-}. On the other hand, the potential of biochar to treat water is compromised by the release of PO_4^{3-} from the biochar. The results show that biochar is removing PO_4^{3-} better at high initial concentration, which increased PO_4^{3-} adsorption. Furthermore, CHC showed the best capability to simultaneously adsorb all nutrients in this study (NH_4^+, NO_3^-, and PO_4^{3-}) from real eutrophic surface water. Although CHC is acidic on the surface, the final pH value was approximately neutral (≈ 7.1), which is acceptable for water treatment. CHC has abundant and versatile functions on its surface. Therefore, CHC can be used as an adsorbent for the simultaneous treatment of the main inorganic nutrients in surface water. Pelletization enables use of this biochar for water filtration, and microbial attachment to the biochar should be investigated in future studies to enhance the nutrient removal in biofiltration processes.

Acknowledgements
The study of T. Thongsmer was sponsored by the Petchra Pra Jom Klao Ph.D. Research Scholarship (No. 53/2561) from King Mongkut's University of Technology Thonburi. Additional support was provided by the Thailand research fund no. RDG6030006 and by the Newton Fund via the Biotechnology and Biological Sciences Research Council of the United Kingdom (BB/P027709/1).

Authors' contributions
Thunchanok Thongsamer conducted experiment and provided data and prepared draft manuscript. Soydoa Vinitnantrarat, Anawat Pinisakul and David Werner provided the conceptualization, supervision and corrected the manuscript. David Werner helped revise English language. All authors read and approved the final manuscript.

Funding
This study was supported by The Petchra Pra Jom Klao Ph.D. Research Scholarship (No. 53/2561) from King Mongkut's University of Technology Thonburi, Bangkok, Thailand.

Availability of data and materials
All data generated or analyzed during this study are presented within the submitted manuscript.

Declarations

Competing interests
The authors declare they have no competing interests.

Author details
[1]Environmental Technology Program, School of Energy, Environment and Materials, King Mongkut's University of Technology Thonburi, Bangkok 10140, Thailand. [2]Environmental and Energy Management for Community and Circular Economy Research Group, King Mongkut's University of Technology Thonburi, Bangkok 10140, Thailand. [3]Chemistry for Green Society and Healthy Research Group, King Mongkut's University of Technology Thonburi, Bangkok 10140, Thailand. [4]School of Engineering, Newcastle University, Newcastle upon Tyne NE1 7RU, UK.

Received: 1 April 2022 Accepted: 17 August 2022
Published online: 05 September 2022

References

1. Dodds WK, Smith VH. Nitrogen, phosphorus, and eutrophication in streams. Inland Waters. 2016;6:155–64.
2. Zeng QH, Qin LH, Bao LL, Li YY, Li XY. Critical nutrient thresholds needed to control eutrophication and synergistic interactions between phosphorus and different nitrogen sources. Environ Sci Pollut R. 2016;23:21008–19.
3. Mrozik W, Vinitnantharat S, Thongsamer T, Pansuk N, Pattanachan P, Thayanukul P, et al. The food-water quality nexus in periurban aquacultures downstream of Bangkok, Thailand. Sci Total Environ. 2019;695:133923.
4. Gelberg KH, Church L, Casey G, London M, Roerig DS, Boyd J, et al. Nitrate levels in drinking water in rural New York State. Environ Res. 1999;80:34–40.
5. Burch MD. Effective doses, guidelines & regulations. In: Hudnell HK, editor. Cyanobacterial harmful algal blooms: state of the science and research needs. New York: Springer; 2008. p. 831–53.
6. Mrozik W, Minofar B, Thongsamer T, Wiriyaphong N, Khawkomol S, Plaimart J, et al. Valorisation of agricultural waste derived biochars in aquaculture to remove organic micropollutants from water – experimental study and molecular dynamics simulations. J Environ Manage. 2021;300:113717.
7. Ahmad M, Rajapaksha AU, Lim JE, Zhang M, Bolan N, Mohan D, et al. Biochar as a sorbent for contaminant management in soil and water: a review. Chemosphere. 2014;99:19–33.
8. Tan XF, Liu YG, Zeng GM, Wang X, Hu XJ, Gu YL, et al. Application of biochar for the removal of pollutants from aqueous solutions. Chemosphere. 2015;125:70–85.
9. Zhang M, Song G, Gelardi DL, Huang LB, Khan E, Masek O, et al. Evaluating biochar and its modifications for the removal of ammonium, nitrate, and phosphate in water. Water Res. 2020;186:116303.
10. Fan RM, Chen CL, Lin JY, Tzeng JH, Huang CP, Dong CD, et al. Adsorption characteristics of ammonium ion onto hydrous biochars in dilute aqueous solutions. Bioresour Technol. 2019;272:465–72.
11. Kizito S, Wu SB, Wandera SM, Guo LC, Dong RJ. Evaluation of ammonium adsorption in biochar-fixed beds for treatment of anaerobically digested swine slurry: experimental optimization and modeling. Sci Total Environ. 2016;563:1095–104.
12. Ahmad M, Ahmad M, Usman ARA, Al-Faraj AS, Abduljabbar AS, Al-Wabel MI. Biochar composites with nano zerovalent iron and eggshell powder for nitrate removal from aqueous solution with coexisting chloride ions. Environ Sci Pollut R. 2018;25:25757–71.
13. Yin QQ, Wang RK, Zhao ZH. Application of Mg-Al-modified biochar for simultaneous removal of ammonium, nitrate, and phosphate from eutrophic water. J Clean Prod. 2018;176:230–40.
14. Novais SV, Zenero MDO, Barreto MSC, Montes CR, Cerri CEP. Phosphorus removal from eutrophic water using modified biochar. Sci Total Environ. 2018;633:825–35.
15. Zhao TT, Feng T. Application of modified chitosan microspheres for nitrate and phosphate adsorption from aqueous solution. RSC Adv. 2016;6:90878–86.

16. Almanassra IW, Mckay G, Kochkodan V, Atieh MA, Al-Ansari T. A state of the art review on phosphate removal from water by biochars. Chem Eng J. 2021;409:128211.
17. Hu Q, Shao JA, Yang HP, Yao DD, Wang XH, Chen HP. Effects of binders on the properties of bio-char pellets. Appl Energ. 2015;157:508–16.
18. Aransiola EF, Oyewusi TF, Osunbitan JA, Ogunjimi LAO. Effect of binder type, binder concentration and compacting pressure on some physical properties of carbonized corncob briquette. Energy Rep. 2019;5:909–18.
19. Khawkomol S, Neamchan R, Thongsamer T, Vinitnantharat S, Panpradit B, Sohsalam P, et al. Potential of biochar derived from agricultural residues for sustainable management. Sustainability-Basel. 2021;13:8147.
20. Zhou XY. Correction to the calculation of Polanyi potential from Dubinnin-Rudushkevich equation. J Hazard Mater. 2020;384:121101.
21. Liu Y. Is the free energy change of adsorption correctly calculated? J Chem Eng Data. 2009;54:1981–5.
22. Lima EC, Hosseini-Bandegharaei A, Moreno-Pirajan JC, Anastopoulos I. A critical review of the estimation of the thermodynamic parameters on adsorption equilibria. Wrong use of equilibrium constant in the Van't Hoof equation for calculation of thermodynamic parameters of adsorption. J Mol Liq. 2019;273:425–34.
23. Aghoghovwia MP, Hardie AG, Rozanov AB. Characterisation, adsorption and desorption of ammonium and nitrate of biochar derived from different feedstocks. Environ Technol. 2022;43:774–87.
24. Ahmad R, Rohim R, Ibrahim N. Properties of waste eggshell as calcium oxide catalyst. Appl Mech Mater. 2015;754–5:171–5.
25. Hu XJ, Zhang XB, Ngo HH, Guo WS, Wen HT, Li CC, et al. Comparison study on the ammonium adsorption of the biochars derived from different kinds of fruit peel. Sci Total Environ. 2020;707:135544.
26. Oliveira FR, Patel AK, Jaisi DP, Adhikari S, Lu H, Khanal SK. Environmental application of biochar: current status and perspectives. Bioresour Technol. 2017;246:110–22.
27. Takaya CA, Fletcher LA, Singh S, Anyikude KU, Ross AB. Phosphate and ammonium sorption capacity of biochar and hydrochar from different wastes. Chemosphere. 2016;145:518–27.
28. Shin J, Choi E, Jang E, Hong SG, Lee S, Ravindran B. Adsorption characteristics of ammonium nitrogen and plant responses to biochar pellet. Sustainability-Basel. 2018;10:1331.
29. Marshall JA, Morton BJ, Muhlack R, Chittleborough D, Kwong CW. Recovery of phosphate from calcium-containing aqueous solution resulting from biochar-induced calcium phosphate precipitation. J Clean Prod. 2017;165:27–35.
30. Piccin JS, Cadaval TRSA, de Pinto LAA, Dotto GL. Adsorption isotherms in liquid phase: experimental, modeling, and interpretations. In: Bonilla-Petriciolet A, Mendoza-Castillo D, Reynel-Avila H, editors. Adsorption processes for water treatment and purification. Cham: Springer; 2017. p. 19–51.
31. Al-Ghouti MA, Da'ana DA. Guidelines for the use and interpretation of adsorption isotherm models: a review. J Hazard Mater. 2020;393:122383.
32. Ray SS, Gusain R, Kumar N. Adsorption equilibrium isotherms, kinetics and thermodynamics. In: Carbon nanomaterial-based adsorbents for water purification. Amsterdam: Elsevier; 2020. p. 101–18.
33. Hu QL, Zhang ZY. Application of Dubinin-Radushkevich isotherm model at the solid/solution interface: a theoretical analysis. J Mol Liq. 2019;277:646–8.
34. Saadi R, Saadi Z, Fazaeli R, Fard NE. Monolayer and multilayer adsorption isotherm models for sorption from aqueous media. Korean J Chem Eng. 2015;32:787–99.
35. Hou J, Huang L, Yang ZM, Zhao YQ, Deng CR, Chen YC, et al. Adsorption of ammonium on biochar prepared from giant reed. Environ Sci Pollut R. 2016;23:19107–15.
36. Fidel RB, Laird DA, Spokas KA. Sorption of ammonium and nitrate to biochars is electrostatic and pH-dependent. Sci Rep-UK. 2018;8:17627.
37. Hsu DL, Lu CY, Pang TR, Wang YP, Wang GH. Adsorption of ammonium nitrogen from aqueous solution on chemically activated biochar prepared from sorghum distillers grain. Appl Sci-Basel. 2019;9:5249.
38. Vu TM, Trinh VT, Doan DP, Van HT, Nguyen TV, Vigneswaran S, et al. Removing ammonium from water using modified corncob-biochar. Sci Total Environ. 2017;579:612–9.
39. Ogata F, Imai D, Kawasaki N. Adsorption of nitrate and nitrite ions onto carbonaceous material produced from soybean in a binary solution system. J Environ Chem Eng. 2015;3:155–61.

Publisher's Note